Supplementary material

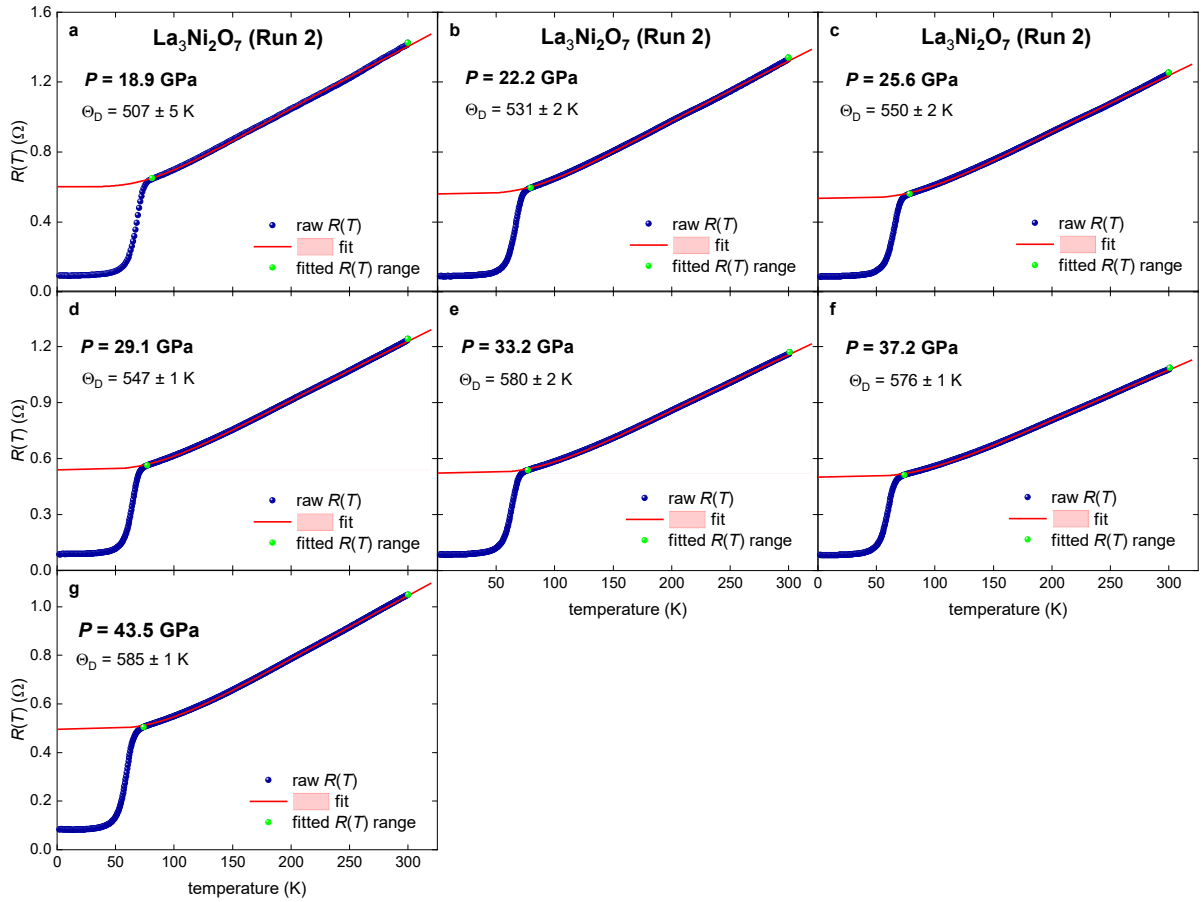

Fig. S1. (Color online) Temperature dependent resistance, $R(T,P)$, measured in compressed single crystal $La_3Ni_2O_7$ (Run 2) and data fits to Eq. (1). Raw data reported by Sun et al [11]. $R_{sat} \to \infty$ for all fits. Green balls indicate the bounds for which $R(T)$ data was used for the fit to Eq. (1). Fit quality for all panels is better or equal to 0.9999. 95% confidence bands are shown by pink areas. P=18.9 GPa (a); P=22.2 GPa (b); P=25.6 GPa (c); P=29.1 GPa (d); P=33.2 GPa (e); P=37.2 GPa (f); P=43.5 GPa (g).

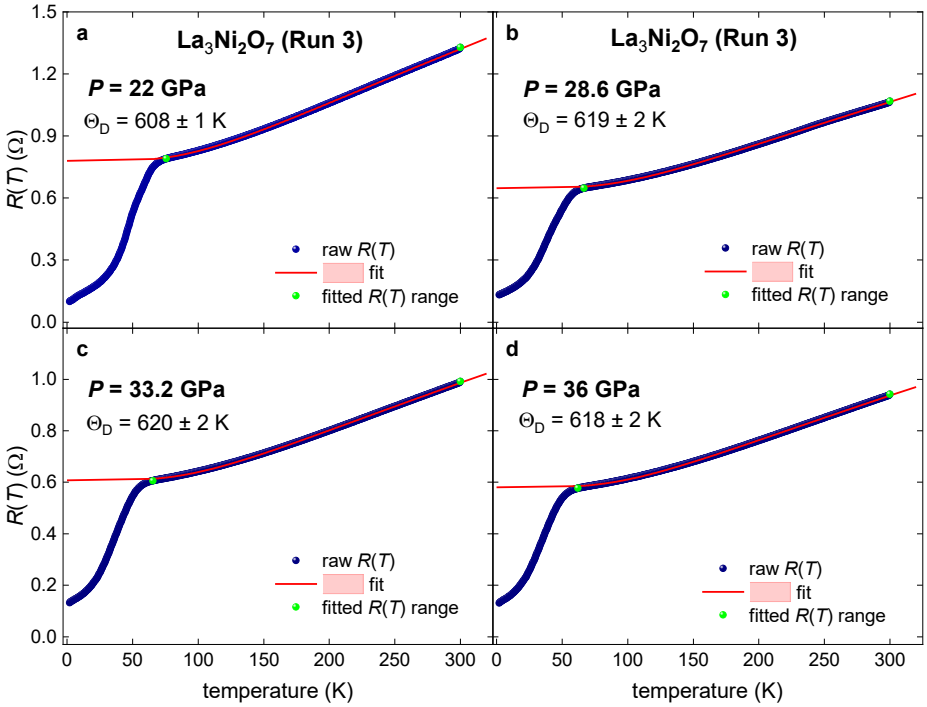

Fig. S2. (Color online) Temperature dependent resistance, $R(T,P)$, measured in compressed single crystal $La_3Ni_2O_7$ (Run 3) and data fits to Eq. (1). Raw data reported by Sun et al [11]. $R_{sat} \to \infty$ for all fits. Green balls indicate the bounds for which $R(T)$ data was used for the fit to Eq. (1). Fit quality for all panels is better or equal to 0.9997. 95% confidence bands are shown by pink areas. P=22 GPa (a); P=28.6 GPa (b); P=33.2 GPa (c); P=36 GPa (d).

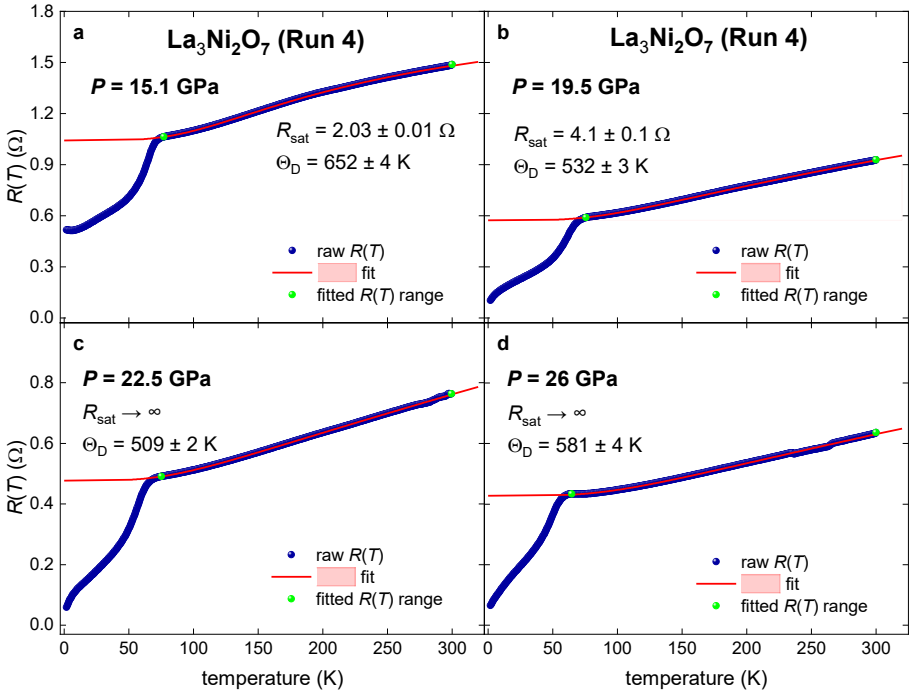

Fig. S3. (Color online) Temperature dependent resistance, $R(T,P)$, measured in compressed single crystal $La_3Ni_2O_7$ (Run 4) and data fits to Eq. (1). Raw data reported by Sun et al [11]. Green balls indicate the bounds for which $R(T)$ data was used for the fit to Eq. (1). Fit quality for all panels is better or equal to 0.9989. 95% confidence bands are shown by pink areas. P=15.1 GPa (a); P=19.5 GPa (b); P=22.5 GPa (c); P=26 GPa (d).

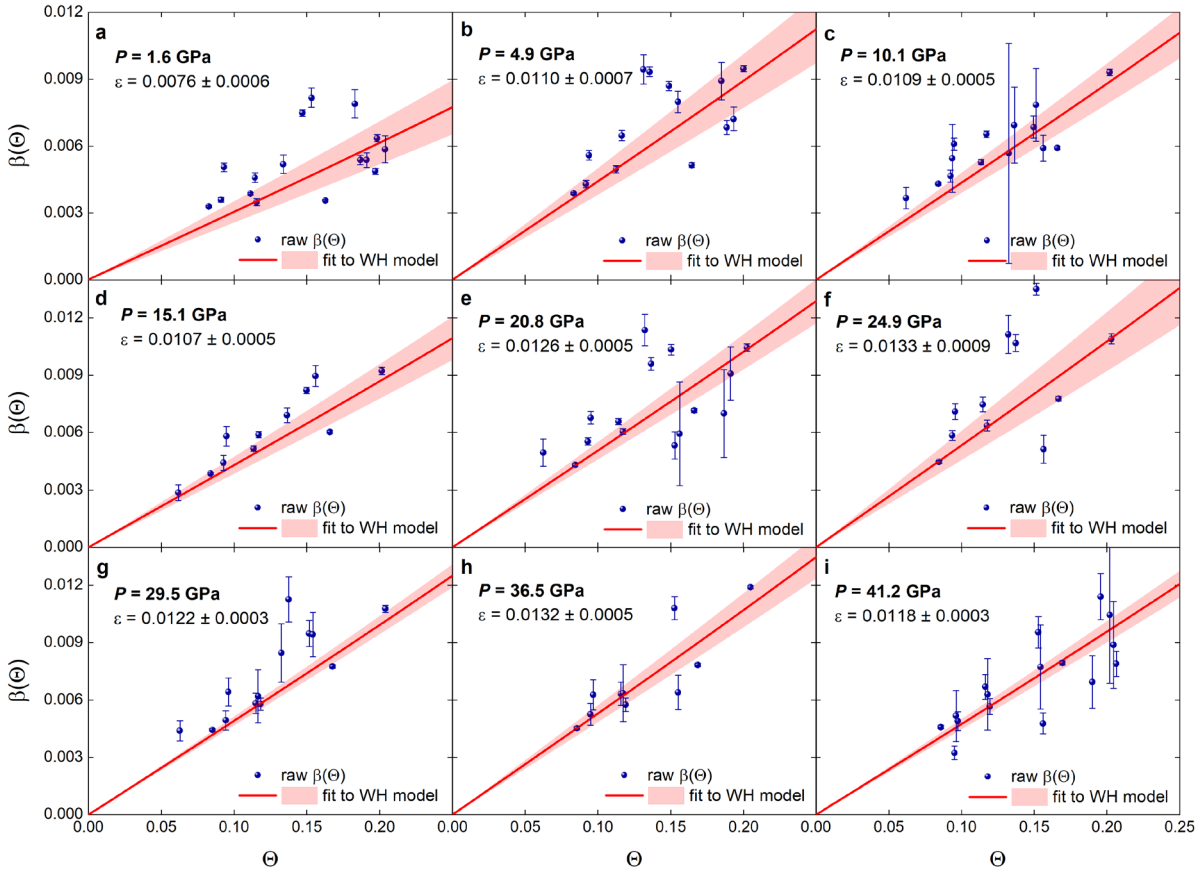

Fig. S4. (Color online) XRD peaks breadth, β(θ), fits to reduced Williamson-Hall model (Eq. (9)) for highly compressed single crystal $La_3Ni_2O_{7-\delta}$. Raw XRD scans reported by Sun et al [11]. 95% confidence bands are shown by pink areas. P=1.6 GPa (a); P=4.9 GPa (b); P=10.1 GPa (c); P=15.1 GPa (d), P=20.8 GPa (e); P=24.9 GPa (f); P=29.5 GPa (g); P=36.5 GPa (h), P=41.2 GPa (i).